Nanostructures

DOI: 10.1002/anie.200902305

Synthesis of Out-of-Substrate Au–Ag Nanoplates with Enhanced Stability for Catalysis**

Yugang Sun and Changhui Lei*

Metal nanoparticles represent an important class of components in many applications, such as catalysis, electronics, optics, optoelectronics, sensing, and data storage, because of their unique properties.[1–11] In principle, the properties of a nanoparticle are determined by various parameters including composition, size, morphology, crystallinity, and surrounding environment, among which morphological control is one of the most powerful means to tune the properties and thus to influence the performance of the nanoparticle in different applications.[1] For example, cubic silver nanoparticles bounded with {100} facets exhibit much higher catalytic capability towards the oxidation of styrene with *tert*-butyl hydroperoxide than silver nanoplates mainly bounded with {111} facets.[12] Therefore, synthesizing metal nanoparticles with well-controlled shapes and well-defined crystalline surfaces becomes critical to enhance their performance in the envisioned applications. An additional challenge is to form stable assemblies of the as-synthesized nanoparticles to expose useful surfaces that are as large as possible.

We have developed an efficient approach to grow high-quality Ag nanoplates on n-type semiconductor substrates (such as GaAs and Si).[13,14] Figure 1a shows the scanning electron microscopy (SEM) image of a typical sample of Ag nanoplates with an average edge length of 485 nm and thickness of 40 nm. Structural characterization indicates that the two basal surfaces of each nanoplate are bounded by {111} facets. All of the Ag nanoplates protrude from the substrate to highly expose their {111} surfaces to the surrounding environment. However, Ag is easily oxidized in ambient environments, which results in limitation of the potential applications of the nanoplates. As a result, the synthesis of nanoplates made of other noble metals (or alloys) that are more resistant to oxidation is important for improving their performance.

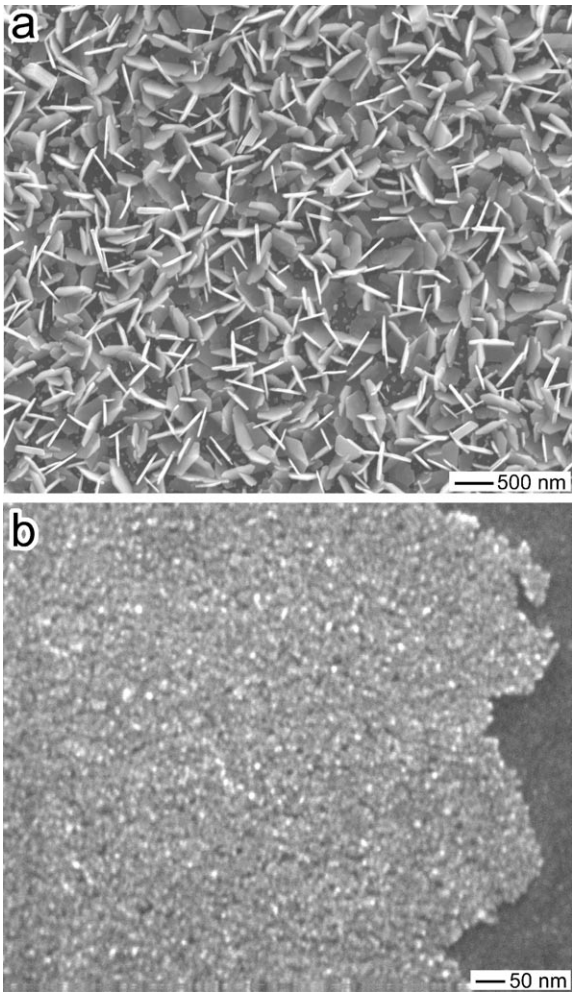

Figure 1. SEM images of a) Ag nanoplates and b) small Au nanoparticles grown on n-type GaAs substrates through reactions with 2 M $AgNO_3$ solution for 4 min and 1 mM $NaAuCl_4$ solution for 10 min, respectively. All the reactions were performed at room temperature (22 °C).

[*] Dr. Y. Sun
Center for Nanoscale Materials, Argonne National Laboratory
9700 South Cass Avenue, Argonne, IL 60439 (USA)
Fax: (+1) 630-252-4646
E-mail: ygsun@anl.gov

Dr. C. Lei
Center for Microanalysis of Materials, Frederick Seitz Materials Research Laboratory, University of Illinois
104 South Goodwin Avenue, Urbana, IL 60801 (USA)

[**] The submitted manuscript was created by UChicago Argonne, LLC, Operator of Argonne National Laboratory ("Argonne"). Argonne, a US Department of Energy Office of Science laboratory, is operated under Contract No. DE-AC02-06CH11357. The US Government retains for itself, and others acting on its behalf, a paid-up, nonexclusive, irrevocable worldwide license in said article to reproduce, prepare derivative works, distribute copies to the public, and perform publicly and display publicly, by or on behalf of the Government. Use of the Center for Nanoscale Materials and the Electron Microscopy Center for Materials Research at Argonne was supported by the US Department of Energy, Office of Science, Office of Basic Energy Sciences, under Contract No. DE-AC02-06CH11357. Characterizations were also carried out by partially using the Center for Microanalysis of Materials Facilities in Frederick Seitz Materials Research Laboratory, University of Illinois, which is partially supported by the US Department of Energy under Grant No. DEFG02-91-ER45439.

Supporting information for this article is available on the WWW under http://dx.doi.org/10.1002/anie.200902305.

The methodology[14] used for growing Ag nanoplates fails to grow nanoplates of other noble metals, such as Au. Instead, only small nanocrystals of Au are deposited with sizes less than 20 nm on GaAs substrates (Figure 1b). Systematic studies reveal that the interdiffusion coefficient between Au and GaAs is much higher than that between Ag and GaAs.[15] The fast interdiffusion is beneficial to the progressive nucleation process of Au nanocrystals during the reactions between Au precursors (e.g., $NaAuCl_4$) and GaAs, which makes it difficult to grow the Au nanocrystals anisotropically into nanoplates. Herein, we report the chemical conversion of as-synthesized Ag nanoplates on GaAs substrates (Figure 1a) into Au–Ag alloy nanoplates, which significantly enhances their stability in applications such as catalysis.

The success of compositional conversion is determined by the unique configuration of the Ag nanoplate/GaAs composite samples, that is, thin layers of oxide (derived from the oxidation of GaAs) cover the surfaces of the GaAs substrates (see the green layer in Figure 2, left).[16] In a typical sample,

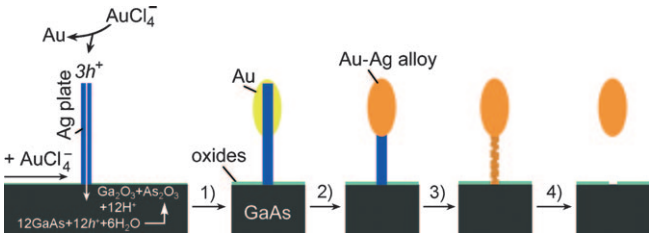

Figure 2. Schematic illustration of the major steps involved in the conversion of Ag nanoplates into Au–Ag alloy nanoplates. For simplicity, the cross-sectional projection of a nanoplate perpendicular to the basal surfaces of a nanoplate is highlighted.

the oxide layer can prevent the interdiffusion process between Au and GaAs, thus eliminating the nucleation and growth of new Au nanocrystals on the GaAs substrate, when the Ag nanoplate/GaAs sample is in contact with the Au precursor (aqueous $NaAuCl_4$ solution). On the other hand, the $AuCl_4^-$ ions can spontaneously oxidize the GaAs substrate and Ag nanoplates through a hole-injection process and galvanic displacement reaction, respectively, at elevated temperatures because the standard reduction potential of the redox pair $AuCl_4^-$/Au (0.994 V vs. standard hydrogen electrode, SHE) is higher than that of Ag^+/Ag (0.7996 V vs. SHE) and those of oxides/GaAs (less than 0.3 V vs. SHE).

Figure 2 illustrates the growth of Au–Ag alloy nanoplates by immersing the sample of Ag nanoplates shown in Figure 1a in an aqueous solution of $NaAuCl_4$ at elevated temperatures. The early stage of the reaction is dominated by oxidation of GaAs with $AuCl_4^-$ ions through the hole-injection process because GaAs exhibits stronger reducing capability than Ag. When a $AuCl_4^-$ ion contacts a Ag nanoplate, it is reduced to a Au atom by releasing three holes, which are injected into the lattice of the GaAs substrate via the Ag nanoplate. The Au atom moves on the surface of the Ag nanoplate to eventually crystallize at a position with the highest surface energy. The continuous hole-injection process leads to the deposition of a Au cap on and around the lateral surfaces (bounded by high-index facets) of the Ag nanoplate, which have higher surface energy than the basal flat {111} surfaces (step 1). The Au coating prevents the underneath silver from directly reacting with $AuCl_4^-$ ions through galvanic displacement. As a matter of fact, silver and gold tend to form a nearly ideal solid solution because the homogeneous Au–Ag alloy is more thermodynamically stable than either pure Au or Ag. As a result, the overgrown Au cap quickly alloys with the underlying silver because the interdiffusion rates between silver and gold are high at high temperatures (step 2).[17] When the Au cap is thick enough, the continuous reaction is dominated by a galvanic displacement reaction between $AuCl_4^-$ ions and the Ag nanoplate over the uncovered, stable {111} basal surfaces followed by alloying and dealloying processes. These sequential processes lead to the formation of a rough Au–Ag alloy wall (step 3). Further reaction leads to the collapse of the thin wall to release a Au–Ag alloy particle from the GaAs substrate (step 4).

Figure 3 shows a series of SEM images of the samples synthesized through reactions between the Ag nanoplates shown in Figure 1a and 1 mM $NaAuCl_4$ aqueous solution at about 90 °C for different times. At the beginning of the reaction, the nanoplates become thicker around their lateral edges to form tapered structures. For instance, the thickness of the nanoplates near the edges increases from 40 to 90 nm when the reaction lasts 30 s (Figure 3a). The surfaces of the nanoplates are still smooth, which indicates that the $AuCl_4^-$ ions do not etch the Ag nanoplates through a galvanic displacement reaction. Therefore, the gold layers are deposited through the hole-injection process, in which the holes are injected into the lattices of the GaAs substrate, followed by alloying. When the reaction continues, the central regions (bounded by {111} facets) of the tapered nanoplates become rough with the appearance of many small pores (Figure 3b). This roughening process is ascribed to the galvanic reaction between $AuCl_4^-$ ions and Ag followed by alloying and dealloying processes.[17] The thickness of the rough areas of the nanoplates can be further decreased to eventually collapse, which results in the release of thick Au–Ag alloy particles with crescent-shaped morphologies from the GaAs substrate if the reaction lasts long enough. The sample shown in Figure 3c is synthesized with a reaction time of 90 s.

The Au–Ag nanoplates shown in Figure 3b are interesting because of their out-of-substrate orientation and alloy compositions, which are more resistant to oxidation than pure Ag. The inset of Figure 3b presents the scanning transmission electron microscopy (STEM) image of an individual nanoplate on a Cu grid coated with a carbon film. The spatial contrast distribution confirms the tapered profile of the nanoplate. Energy-dispersive X-ray spectroscopic (EDS) analysis shows that the nanoplate is composed of only Au and Ag. The absence of signals for Ga and As indicates that the interdiffusion between GaAs and Ag–Au is prevented because of the existence of the oxide layers. Quantitative analysis over multiple spots along a line across the nanoplate shows that the compositions at these spots are similar with average values of 24.6% for Ag and 75.4% for

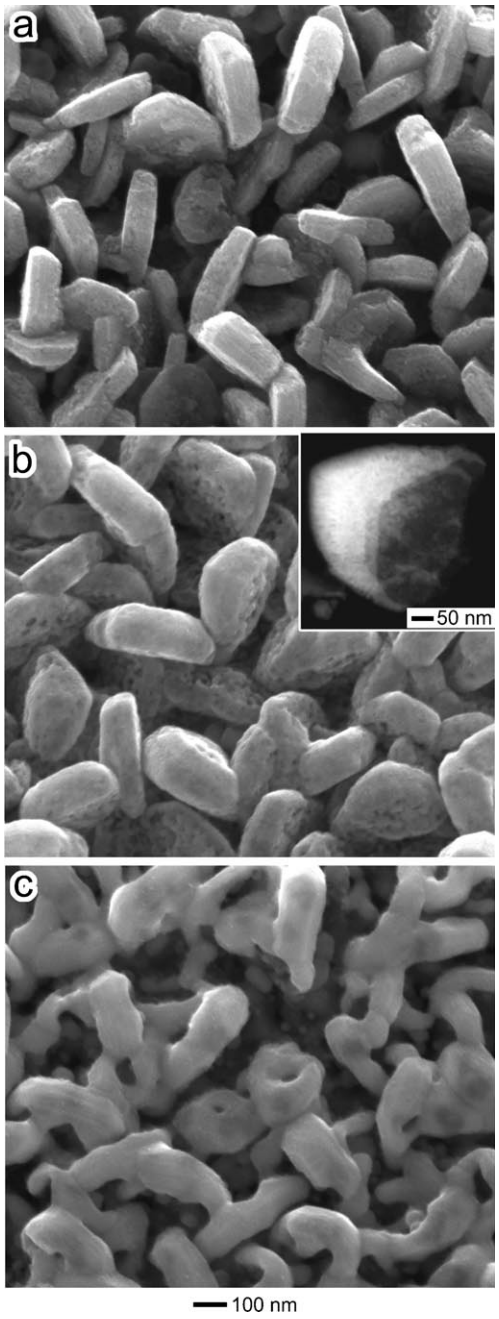

Figure 3. SEM images of the samples obtained through reaction between the Ag nanoplates shown in Figure 1a and 1 mM $NaAuCl_4$ solution at 90 °C for a) 30, b) 60, and c) 90 s.

Au (see the Supporting Information, Figure S1). The compositions and morphologies of the nanoplates are significantly influenced by the reaction temperature and time. For example, reactions at room temperature (22 °C) lead to the deposition of AgCl because of the low dissolvability of AgCl at low temperatures (see the Supporting Information, Figure S2). In addition, the thicknesses of the nanoplates do not change, with no apparent increase even after reaction with $AuCl_4^-$ for 1 min. These results indicate that reactions between Ag nanoplates and $AuCl_4^-$ ions at low temperatures prefer to follow the direct galvanic displacement process rather than the hole-injection process.

The as-synthesized Au–Ag alloy nanoplates inherit the out-of-substrate orientation of the original Ag nanoplates, which highly expose their surfaces to the surrounding environment. The compositional change from pure Ag to Au–Ag alloy significantly enhances the chemical stability of the nanoplates when they are used in applications such as catalysis. For example, freshly synthesized Ag nanoplates on GaAs substrates exhibit good catalytic ability to accelerate the reduction of 4-nitrophenol (4-NP) with $NaBH_4$ (see the Supporting Information, Figure S3).[18–20] The derived Au–Ag alloy nanoplates show a similar catalytic performance (Figure 4a). The absorption peak at 400 nm (corresponding to the characteristic feature of 4-NP) constantly decreases and the peak at 295 nm increases with reaction time, which indicates the reduction of 4-NP to 4-aminophenol (4-AP). The reduction does not occur without the assistance of the metal

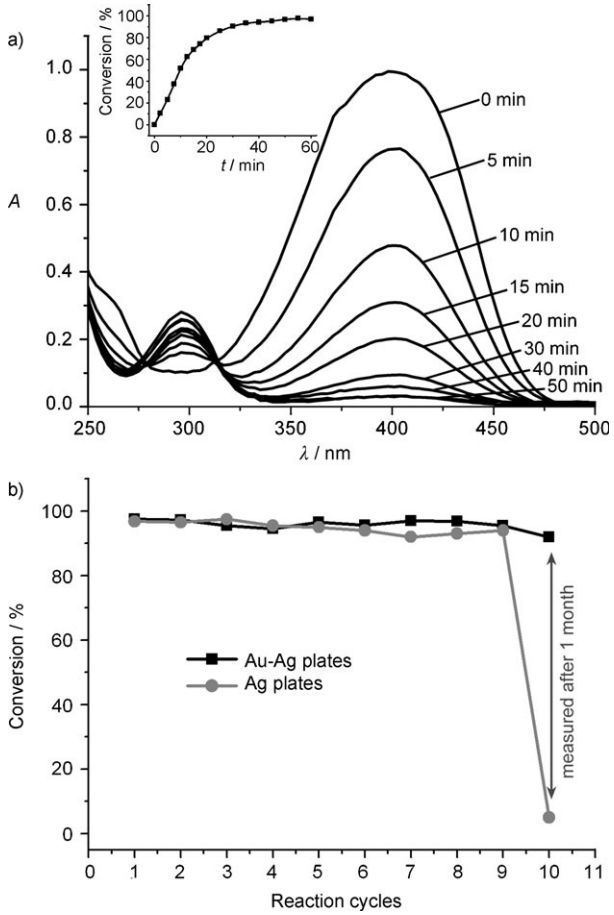

Figure 4. a) UV/Vis spectra of 4-NP measured at different times during its reduction catalyzed by the Au–Ag alloy nanoplates shown in Figure 3b. Inset: dependence of conversion yield of 4-NP to 4-AP on the reaction time. b) Maximum conversion yield of 4-NP in nine successive cycles of reduction with different catalysts: (■) Au–Ag alloy nanoplates and (●) Ag nanoplates. The tenth cycle was measured after the nanoplates had been stored for 1 month in an ambient environment.

nanoplates under the same reaction conditions. Since these nanoplates are fixed on the substrates, they can be easily recovered to catalyze additional reactions.

As shown in Figure 4b, both freshly prepared Ag nanoplates and Au–Ag alloy nanoplates can catalyze the reduction of 4-NP for many successive cycles with similar conversion yields near 100%. After storing the samples in an ambient environment for 1 month, the pure Ag nanoplates essentially lose catalytic capability as a result of oxidation to silver oxide. In contrast, the Au–Ag alloy nanoplates with a high concentration of Au (e.g., ca. 75% Au and ca. 25% Ag; Figure 3b) can still efficiently catalyze the reduction of 4-NP although the conversion yield slightly decreases by several percent. This obvious difference indicates that converting the Ag nanoplates into Au–Ag alloy nanoplates significantly increases their resistance towards oxidation in an ambient environment. Nanoplates made of Au–Ag alloys with Au concentrations higher than about 60% withstood oxidation in air and retained their catalytic ability.

In conclusion, Ag nanoplates grown on GaAs substrates have been successfully converted into chemically stable nanoplates made of Au–Ag alloys. These alloy nanoplates retain the out-of-substrate orientation and highly expose their surfaces to surrounding solutions for efficient catalysis. This synthetic strategy can be extended to the preparation of Pd–Ag and Pt–Ag alloy nanoplates by using appropriate precursors (e.g., Na_2PdCl_4 for Pd–Ag and Na_2PtCl_4 for Pt–Ag; see the Supporting Information, Figure S4). The alloy nanoplates derived from high-quality Ag nanoplates can serve as reusable catalysts with enhanced stability and efficiency.

Experimental Section

Synthesis of metal nanoplates: Ag nanoplates on n-type GaAs wafers doped with Si at a concentration of about $1\times10^{18}\,cm^{-3}$ (AXT, Fremont, CA) were grown by following the procedure described elsewhere.[14] In a typical process, a droplet (ca. 20 μL) of 2 M $AgNO_3$ (Aldrich) aqueous solution was delivered to an approximately $0.7\times0.7\,cm^2$ clean GaAs wafer. Reaction for 4 min in the dark and under ambient conditions produced Ag nanoplates as shown in Figure 1a. The GaAs wafer covered with Ag nanoplates was then immersed in $NaAuCl_4$ solution (10 mL, 1 mM; Aldrich) heated at different temperatures to convert the Ag nanoplates into Au–Ag alloy nanoplates. The reaction was terminated by removing the sample from the solution and rinsing with deionized (DI) water.

Characterization: SEM images were obtained on a Quanta 400F (FEI) microscope operated at 20 kV in the high-vacuum mode. STEM and EDS analysis were performed on a JEOL 2010F transmission electron microscope equipped with an EDS detector (Oxford). The microscope was operated at 200 kV for all of the characterizations.

Catalytic reduction of 4-NP: In a typical reaction, aqueous solutions of 4-NP (0.01 mL, 0.01M) and $NaBH_4$ (0.20 mL, 0.1M) were mixed with DI water (1 mL) in a cuvette. A piece of GaAs wafer covered with metal nanoplates was then immersed in the solution. Changes in the absorption spectra of the solution were monitored with a spectrometer (Perkin–Elmer). The solution was shaken throughout the reaction. After each reaction was completed, the GaAs substrate was removed from the solution and dried by blowing with N_2. The nanoplate/GaAs sample was rinsed with plenty of water and dried with N_2 before it was stored. The dried nanoplates could be used to catalyze additional reactions.

Received: April 29, 2009
Published online: August 17, 2009

Keywords: alloys · gold · heterogeneous catalysis · nanoplates · silver

[1] Y. Xia, Y. Xiong, B. Lim, S. E. Skrabalak, *Angew. Chem.* **2009**, *121*, 62; *Angew. Chem. Int. Ed.* **2009**, *48*, 60.
[2] Y. Xiong, B. J. Wiley, Y. Xia, *Angew. Chem.* **2007**, *119*, 7291; *Angew. Chem. Int. Ed.* **2007**, *46*, 7157.
[3] N. Tian, Z.-Y. Zhou, S.-G. Sun, Y. Ding, Z. L. Wang, *Science* **2007**, *316*, 732.
[4] A. R. Tao, S. Habas, P. Yang, *Small* **2008**, *4*, 310.
[5] S. Yang, Z. Peng, H. Yang, *Adv. Funct. Mater.* **2008**, *18*, 2745.
[6] S. Jeong, K. Woo, D. Kim, B. Lim, J. S. Kim, H. Shin, Y. Xia, J. Moon, *Adv. Funct. Mater.* **2008**, *18*, 679.
[7] C. B. Murray, S. Sun, H. Doyle, T. Betley, *MRS Bull.* **2001**, *26*, 985.
[8] T. A. Taton, C. A. Mirkin, R. L. Letsinger, *Science* **2000**, *289*, 1757.
[9] X. Zhang, M. A. Young, O. Lyandres, R. P. Van Duyne, *J. Am. Chem. Soc.* **2005**, *127*, 4484.
[10] J. L. West, N. J. Halas, *Annu. Rev. Biomed. Eng.* **2003**, *5*, 285.
[11] C. J. Murphy, A. M. Gole, J. W. Stone, P. N. Sisco, A. M. Alkilany, E. C. Goldsmith, S. C. Baxter, *Acc. Chem. Res.* **2008**, *41*, 1721.
[12] R. Xu, D. Wang, J. Zhang, Y. Li, *Chem. Asian J.* **2006**, *1*, 888.
[13] Y. Sun, *Chem. Mater.* **2007**, *19*, 5845.
[14] Y. Sun, H. Yan, G. P. Wiederrecht, *J. Phys. Chem. C* **2008**, *112*, 8928.
[15] S. Y. Sayed, B. Daly, J. M. Buriak, *J. Phys. Chem. C* **2008**, *112*, 12291.
[16] Y. Sun, C. Lei, D. Gosztola, R. Haasch, *Langmuir* **2008**, *24*, 11928.
[17] Y. Sun, Y. Xia, *J. Am. Chem. Soc.* **2004**, *126*, 3892.
[18] Y. Lu, Y. Mei, M. Drechsler, M. Ballauff, *Angew. Chem.* **2006**, *118*, 827; *Angew. Chem. Int. Ed.* **2006**, *45*, 813.
[19] J. Lee, J. C. Park, H. Song, *Adv. Mater.* **2008**, *20*, 1523.
[20] Q. Zhang, T. Zhang, J. Ge, Y. Yin, *Nano Lett.* **2008**, *8*, 2867.

